

Analysis of Spectral Notching in FM Noise Radar Using Measured Interference

Brandon Ravenscroft^{1*}, Shannon D. Blunt¹, Chris Allen¹, Anthony Martone² and Kelly Sherbondy²

¹University of Kansas – Radar Systems Lab, Lawrence, KS, USA; * g171r597@ku.edu

²U.S. Army Research Laboratory, Adelphi, MD, USA

Keywords: Cognitive Radar, Spectral Notching, FM Noise Radar

Abstract

It was recently shown that spectral notches can be incorporated into a physically realizable form of FM noise radar. Here it is shown how these spectral notches can be used to permit radar operation in a band where narrowband interference sources are present. The impact of interference and associated notches in different regions of the waveform spectrum (i.e. passband versus roll-off regions) is examined through assessment of the matched filter response when considering different receive power levels for the radar relative to measured interference. This assessment is performed for both simulated and experimentally measured notched waveforms.

1 Introduction

Auctioning of frequency bands once designated solely for radar use [1] severely undermines the performance of vital sensing functions. These radar systems must therefore either move to other bands, a prospect that is extremely costly and involves less desirable electromagnetic propagation and phenomenology [2], or learn how to cohabitate with other spectrally congested RF systems via a cognitive framework (e.g. [3,4]). This rapidly increasing spectral congestion has necessitated the investigation of how radar systems may better operate in a crowded spectrum by minimizing interference to other users and vice-versa.

Here we explore a means to avoid spectral interference by placing spectral notches in a form of FM noise radar denoted as pseudo-random optimized (PRO), for which FMCW [5] and pulsed FM [6] versions have been realized. This waveform is attractive because it is constant amplitude and well-contained spectrally, thus making it amenable for use with a high-power radar transmitter. Further, while it is known that range sidelobes will degrade when spectral notches are incorporated into a waveform [7], the non-repeated structure of PRO-FMCW provides inherent robustness to this effect due to the non-coherence of sidelobes across waveform segments in the coherent processing interval (CPI), and likewise for the pulsed PRO-FM case. It was shown in [8,9] that spectral notches can be readily incorporated into the waveform design process without adversely affecting physical realizability. In [10] it was even demonstrated that a multi-function radar/communication

capability can be achieved via a tandem hopping arrangement. To assess the robustness to in-band/adjacent-band interference, measured data collected at the U.S. Army Research Laboratory (ARL) is used to synthetically assess the pulse compression filter response for different combinations of both simulated and physically measured notched PRO-FMCW waveforms and measured interference at various power levels and relative spectral locations.

2 Spectrum Shaping and Optimization

The PRO-FMCW waveform [5] is designed on a segment-by-segment basis with pseudo-random initializations and subsequent optimization to approximate a desired power spectrum $|G(f)|^2$ (a Gaussian shape is an attractive choice because it corresponds to low range sidelobes). Because each segment is initialized with a random FM waveform, the result after spectral-shaping optimization of each segment retains a unique range sidelobe structure that, when combined across segments during Doppler processing, further reduces the sidelobes to yield a thumbtack delay-Doppler ambiguity function.

Spectral notches were introduced into the PRO-FMCW framework in [8] through enforcement of

$$|G(f)|=0 \text{ for } f \in \Omega, \quad (1)$$

where Ω represents the set of frequency interval(s) for the spectral notches. It was noted in [8] that inclusion of spectral notches with sharp edges produce a $\sin(x)/x$ roll-off of the range sidelobes. This effect was partially mitigated [9] through tapering of the notch edges to allow for a gradual transition as

$$|G(f)| = \begin{cases} h_L(f) & \text{for } f \in \Omega_L \\ 0 & \text{for } f \in \Omega \\ h_U(f) & \text{for } f \in \Omega_U \end{cases}, \quad (2)$$

where Ω_L , Ω , and Ω_U correspond to the frequency intervals of the lower frequency taper, the notch, and the upper frequency taper, respectively. The frequency tapers $h_L(f)$ and $h_U(f)$ are forced to be continuous with the surrounding power spectrum, thus providing a gradual transition.

Initialization and optimization of a set of M unique segments comprises the total PRO-FMCW waveform. Prior to optimization, the m th segment is initialized with a length T pseudo-random FM signal $p_{0,m}(t)$ taken from a random instantiation of the polyphase-code FM (PCFM) framework [11]. The m th segment of the PRO-FMCW waveform, denoted as $p_{K,m}(t)$, is then generated by K iterations of the alternating projections

$$r_{k+1,m}(t) = \mathbb{F}^{-1} \left\{ |G(f)| \exp \left(j \angle \mathbb{F} \left\{ p_{k,m}(t) \right\} \right) \right\} \quad (3)$$

and

$$p_{k+1,m}(t) = u(t) \exp \left(j \angle r_{k+1,m}(t) \right), \quad (4)$$

where $u(t)$ is a length T rectangular window to maintain constant amplitude, $\angle(\bullet)$ extracts the phase of the argument, \mathbb{F} is the Fourier transform, and \mathbb{F}^{-1} is the inverse Fourier transform.

Notch depths of about 20 dB relative to the local power spectrum peak can be obtained through application of the notch regions defined in (1) and (2) to the formulation in (3). However, greater notch depths are required to adequately mitigate spectral interference (and to not interfere with other spectrum users). Deeper notches can be obtained via the Reiterative Uniform Weighting Optimization (RUWO) method [12], where the optimized m th segment $p_{k,m}(t)$ is cast as the length- N discretized vector $\mathbf{x}_{0,m}$ corresponding to temporal extent T and over-sampled with respect to 3-dB bandwidth B to represent the power spectrum with sufficient fidelity.

Per [8], the frequency sets in Ω from (1) are discretized into Q frequency values f_q . An $N \times Q$ matrix of frequency steering vectors is then defined as

$$\mathbf{B} = \begin{bmatrix} 1 & 1 & \dots & 1 \\ e^{j2\pi f_0} & e^{j2\pi f_1} & \dots & e^{j2\pi f_{Q-1}} \\ \vdots & \vdots & & \vdots \\ e^{j2\pi f_0(N-1)} & e^{j2\pi f_1(N-1)} & \dots & e^{j2\pi f_{Q-1}(N-1)} \end{bmatrix}. \quad (5)$$

The structured $N \times N$ interference covariance matrix is subsequently formed via

$$\mathbf{W} = \mathbf{B}\mathbf{B}^H + \delta\mathbf{I}, \quad (6)$$

where δ is a diagonal loading term and \mathbf{I} is an $N \times N$ identity matrix. After the K iterations of (3) and (4), applying L iterative applications of

$$\mathbf{x}_{l,m} = \exp \left(j \angle \left(\mathbf{W}^{-1} \mathbf{x}_{l-1,m} \right) \right) \quad (7)$$

produces deeper notches, where the resulting vector $\mathbf{x}_{L,m}$ can be readily converted into the continuous time signal $x_{L,m}(t)$ due to the sufficient over-sampling. After the above optimization process, the m th segment is phase rotated so that its initial phase value is identical to the final phase value of the $(m-1)$ th segment to prevent phase discontinuities.

3 Measured Interference Data

Now consider the situation where a radar system must operate in a crowded spectrum while minimizing interference to/from other users. If the spectral notch enforced in (1) and (2) can be made sufficiently deep, the radar can transmit in the crowded spectrum while avoiding interference to other systems. A Gaussian-shaped power spectrum combined with the non-repeating nature of PRO-FMCW yields low autocorrelation sidelobes. It remains to be seen, however, what the impact to radar receive processing will be when such in-band/adjacent-band interference is present.

Here we use spectral data measured from 100 MHz to 1 GHz collected at the Army Research Laboratory (ARL) in Adelphi, MD, USA as described in [3]. The strongest interference source in the data (of -28 dBm at 389 MHz) was chosen to represent a narrowband interference source (see Fig. 1). In the following simulations, this measured interference source and surrounding noise level are synthetically combined with both simulated and experimentally measured notched PRO-FMCW waveforms to evaluate the efficacy of such waveforms for interference rejection in a variety of arrangements. Note that, because the interference and radar echoes are uncorrelated, a 12-bit receive ADC would be sufficient to ensure the thermal noise adequately exceeds the quantization noise such that the radar echoes could be captured without the interference saturating the receiver [13-15].

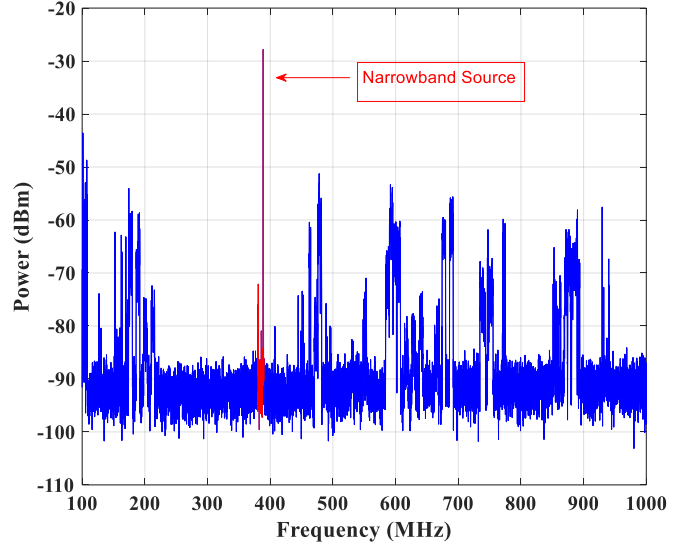


Fig. 1. Measured spectrum (blue) and selected narrowband interference (red)

4 Assessment with Simulated FM Noise

The narrowband interference source in Fig. 1 is used to construct four different interference scenarios by placing the interference in three separate spectral locations relative to the PRO-FMCW waveform baseband spectrum. These locations are shown in Fig. 2. One scenario contains the interference at location A only, one at location B only, one at location C only, and the final contains interference at all three locations.

Four PRO-FMCW transmit waveforms are generated in total, one for each interference scenario. Each PRO-FMCW waveform consists of $M = 10^4$ segments, with each optimized segment having an approximate time-bandwidth product of $BT \cong 1600$, yielding $BT \cong 1.6 \times 10^7$ over the entire M segments (for a coherent integration gain of ~ 72 dB).

For a peak transmit power of 0 dBm, the PRO-FMCW waveform for each case is designed such that the notch depth reaches the measured noise floor to avoid interference with other spectrum users. Note that this transmit power clearly corresponds to a low-power system and there are practical limitations to notch depth (e.g. see [9]) when operating in a high-power regime as discussed in Section 6.

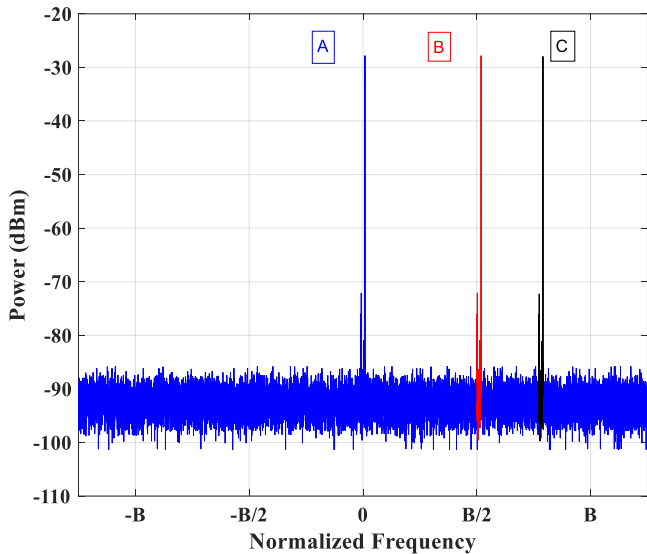


Fig. 2. Constructed interference spectrum locations relative to PRO-FMCW baseband spectrum

A notch of bandwidth $B/16$ is placed in the PRO-FMCW waveform spectrum centered on each interference source (see Fig. 3). Per (2) from [9], a spectral taper of bandwidth $B/16$ is also placed in the transition regions of each notch to minimize the growth of range sidelobes due to sharp spectral notches.

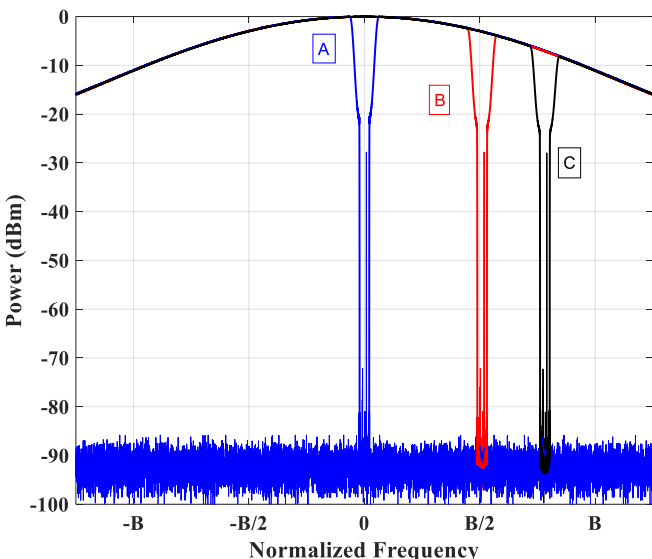


Fig. 3. Simulated notch-tapered PRO-FMCW spectra

To perform the simulated evaluation, a time-domain version of each interference + noise spectrum is superimposed with an attenuated version of the time-domain notched PRO-FMCW waveform to represent the received signal at the radar. The attenuation sets the peak spectral power of the received radar waveform to one of three different power levels: -80 , -100 , and -120 dBm (representing two-way path losses relative to 0 dBm). The reference radar waveform is used to match filter this combined received response to evaluate the impact of the interference and notching. A matched filter result for a PRO-FMCW waveform without notches at each power level is also included for comparison.

The matched filter responses for interference location A are shown in Fig. 4. Clearly the presence of the notch in the middle of the band results in an extended roll-off in range sidelobes compared to the absence of a notch. However, when the relative received radar signal power is low (-100 and -120 dBm) the sidelobe floor is much lower (by roughly 34 dB for both cases) when the transmit waveform avoids the interference through spectral notching. For a higher relative receive power (-80 dBm), the near-in sidelobes of the notched waveforms are much higher than that exhibited by the associated no-notch case, though beyond roughly $0.05T$ the benefit of the notch is still noted (about 27 dB lower).

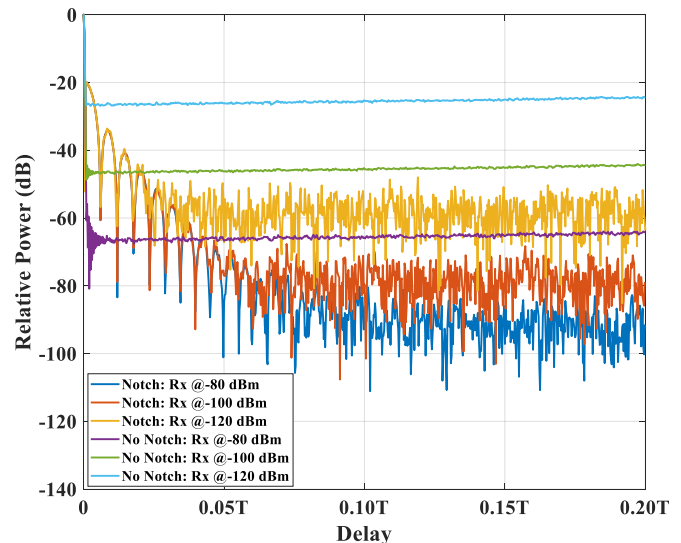


Fig. 4. Matched filter responses (detail view) with interference at location A using simulated PRO-FMCW waveforms

The responses for interference location B are shown in Fig. 5. For the interference/notch midway into the roll-off region (3 dB down from the peak per Fig. 3) the degradation for the no-notch cases are somewhat lessened. However, significant improvements are still observed for the notched waveforms (27 dB for $-120/-100$ dBm and 20 dB for -80 dBm).

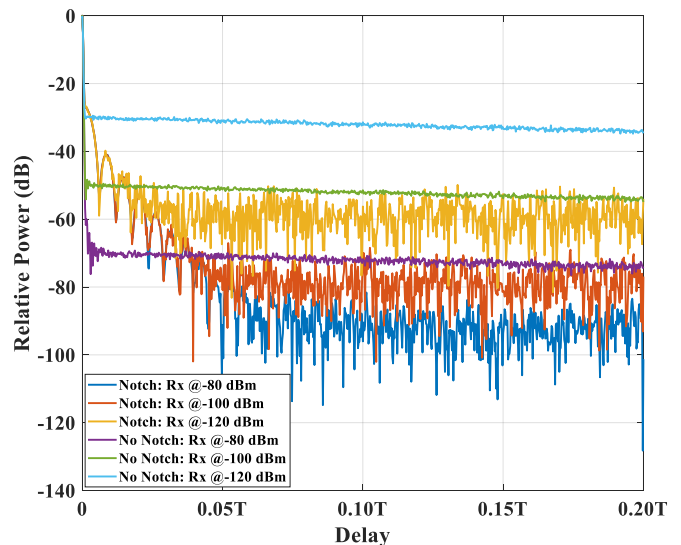


Fig. 5. Matched filter responses (detail view) with interference at location B using simulated PRO-FMCW waveforms

The matched filter response for interference location C is shown in Fig. 6. When the interference is even further into the roll-off region (now 6 dB down from the peak per Fig. 3) there is even less degradation to the matched filter responses than what was observed in the previous two cases (now 25 dB for $-120/-100$ dBm and 18 dB for -80 dBm). The take away from these results is that if spectral notching is employed, it is preferable for it to occur further from the passband if possible. Note that Figs. 4, 5, and 6 are close-up views near the autocorrelation mainlobe and the notched PRO-FMCW waveform for all cases provides the same low sidelobe levels beyond $0.2T$.

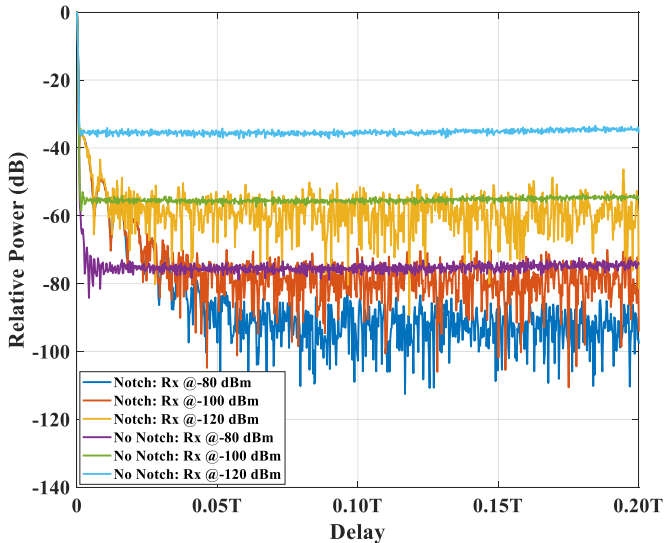


Fig. 6. Matched filter responses (detail view) with interference at location C using simulated PRO-FMCW waveforms

Finally, the matched filter response for interference located in all three locations (A, B, and C) is shown in Fig. 7. With three spectral notches, a significant amount of power is being relocated to the roll-off region of the spectrum (since the waveform is constant amplitude, the total amount of power is fixed), thus increasing the matched filter sidelobes somewhat further. Comparing to Fig. 4 it is observed that the interference/notch in the center of the band is still the dominant factor.

5 Assessment with Measured FM Noise

Now consider physically measured versions of the four notched PRO-FMCW waveforms from Fig. 3 (one for each interference location individually and one for all three simultaneously). Experimentally generating each of these waveforms and capturing in a loopback configuration on hardware highlights the challenges of obtaining sufficient spectral notch depth for real radar waveforms.

Each PRO-FMCW waveform has a length of $T_w = 200$ ms and is comprised of $M = 10^4$ segments. Each segment has a post-optimization 3 dB bandwidth of $B = 80$ MHz and is $T = 20$ μ s in length. As with the simulated waveforms, each experimentally generated, optimized waveform segment has an approximate time-bandwidth product of $BT \cong 1600$, yielding $BT \cong 1.6 \times 10^7$ over the entire M segments. Each

waveform is upsampled to 8 GS/s, converted to a center frequency of 3.55 GHz, and physically generated using a Tektronix AWG70002A arbitrary waveform generator. Each waveform is then subsequently captured in a loopback configuration using a Rohde & Schwarz FSW Real-time Spectrum Analyzer (RSA) at a sampling rate of 200 MS/s.

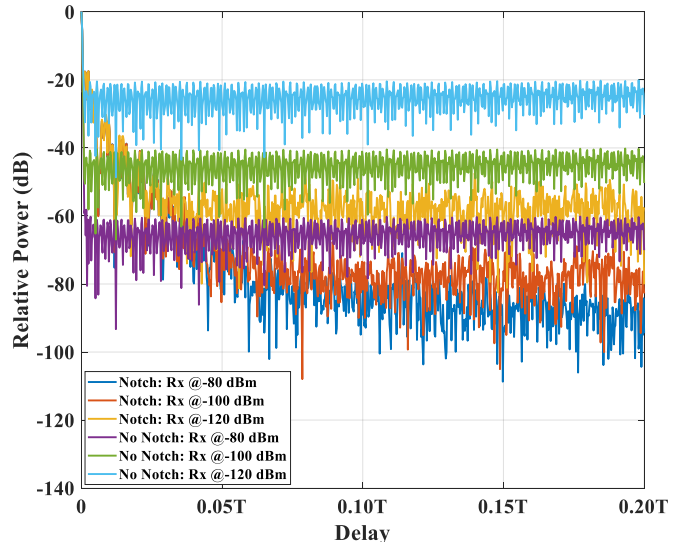


Fig. 7. Matched filter responses (detail view) with interference in all three locations using simulated PRO-FMCW waveforms

The spectra of these experimentally generated and captured waveforms are shown in Fig. 8 along with the same constructed interference spectra from Fig. 2. The RSA has an analysis bandwidth limitation of 160 MHz, which induces a sharp roll-off in the captured spectrum (note the sharper band edges in Fig. 8 relative to Fig. 3). It is now observed that each spectral notch has an achievable depth of only about 42-45 dB relative to the peak due to practical hardware limitations, similar to what was observed in [9]. Since the spectral notches no longer reach the measured noise floor, one can expect this more practical radar emission to impose more interference on other spectrum users.

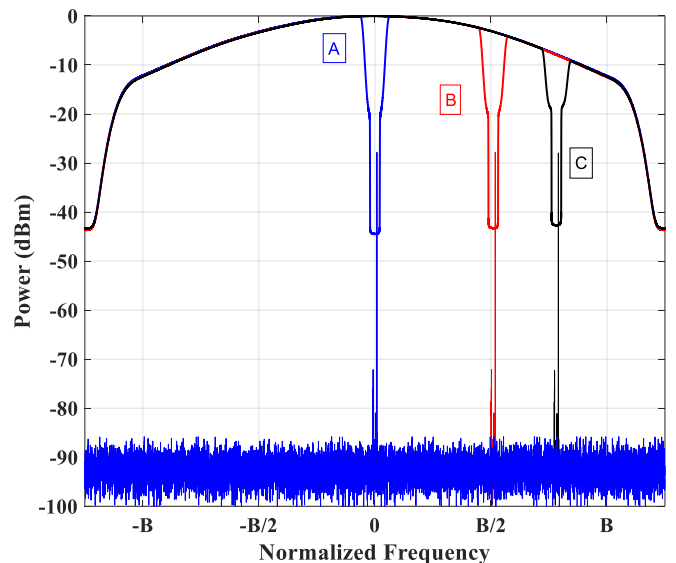


Fig. 8. Physically measured notch-tapered PRO-FMCW spectra

The simulations from the previous section are repeated with the same interference locations and relative receive powers. However, the simulations are now conducted using the measured notched PRO-FMCW waveforms of Fig. 8 instead of simulated PRO-FMCW waveforms. Matched filter results for each simulation scenario using measured waveforms are shown in Figs. 9-12.

The matched filter responses for interference location A are shown in Fig. 9. The plot compares well to its counterpart in Fig. 4, where once again placing a spectral notch in the center of the band induces an extended roll-off of range sidelobes. Nonetheless, similar benefits in the matched filter responses are observed for the notched waveforms which avoid the spectral interference, albeit now with a reduced notch depth. For the -120 , -100 , and -80 dBm cases, these practical notches now provide improvements of 29, 29, and 20 dB, respectively, in the sidelobe floor regions.

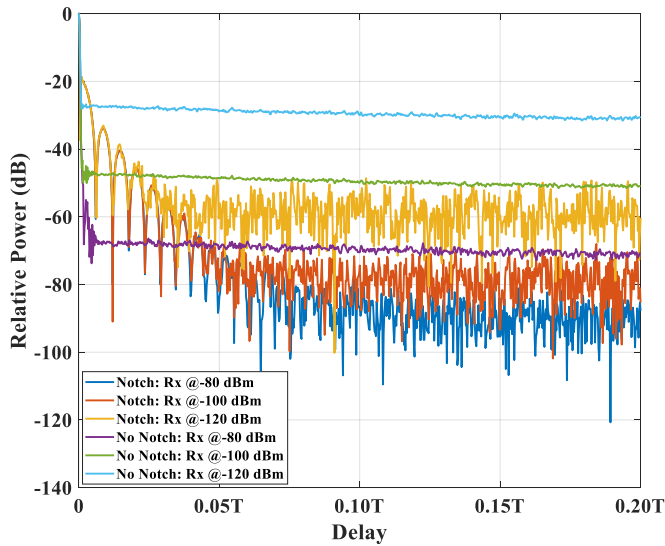


Fig. 9. Matched filter responses (detail view) with interference at location A using measured PRO-FMCW waveforms

The matched filter responses for interference location B are shown in Fig. 10. This plot likewise compares well to its counterpart in Fig. 5. An improvement is once again observed for the range sidelobe roll-off of the matched filter responses of the notched waveforms when the interference/notch is moved further into the spectral roll-off region. At the sidelobe floor, the notches now provide 27, 27, and 19 dB lower sidelobes for the -120 , -100 , and -80 dBm cases, respectively.

The matched filter response for interference location C is shown in Fig. 11. As with the other cases, this plot compares well to its counterpart in Fig. 6. Moving the interference/notch even further into the roll-off region lessens the degradation to the matched filter response. Here the -120 , -100 , and -80 dBm cases yield 25, 25, and 18 dB lower sidelobes. As with the simulated waveforms, the take away is that if spectral notching is employed, it is preferable for it to occur further from the passband.

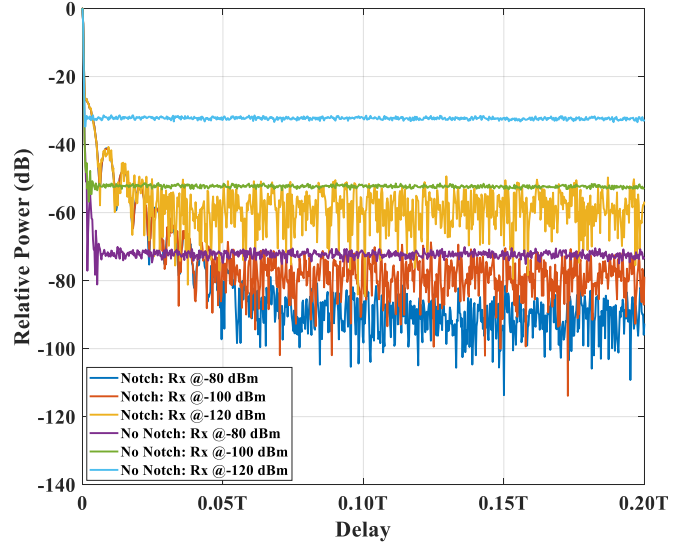


Fig. 10. Matched filter responses (detail view) with interference at location B using measured PRO-FMCW waveforms

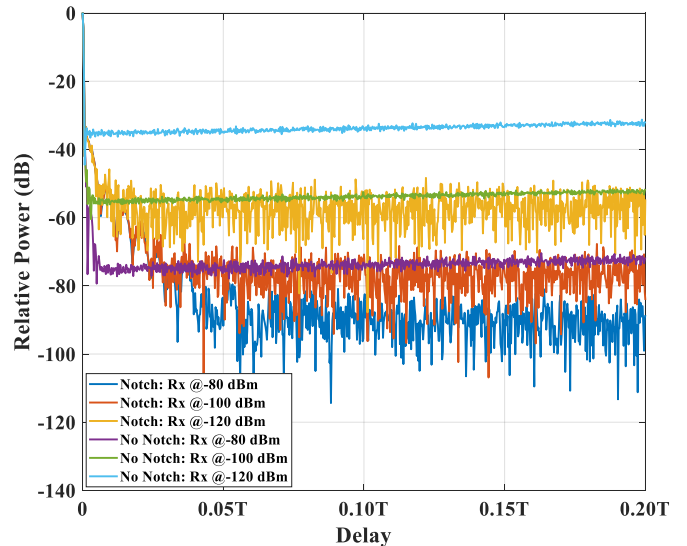


Fig. 11. Matched filter responses (detail view) with interference at location C using measured PRO-FMCW waveforms

Finally, the matched filter response for interference located in all three locations (A, B, and C) is shown in Fig. 12. Comparing to Fig. 7 it is once again observed that interference/notch in the center of the band is the dominant effect since this location corresponds to the peak of the spectral power.

Note that the matched filter results using measured notched PRO-FMCW waveforms are all rather close to their corresponding simulated waveform matched filter results, even though the measured spectral notches are considerably shallower (by more than 40 dB). This observation indicates that spectral notching provides a significant advantage even when the interference cannot be completely mitigated. Of course, other spectral users will experience more interference due to this shallower (practical) notch depth.

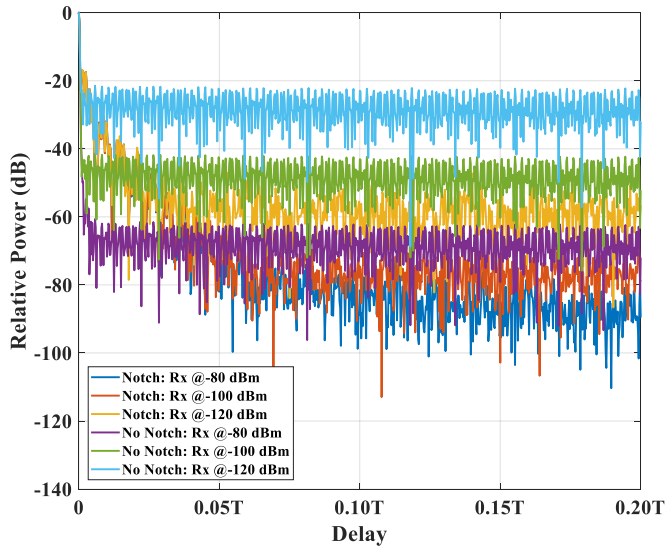


Fig. 12. Matched filter responses (detail view) with interference in all three locations using measured PRO-FMCW waveforms

6 Practical Considerations

The synthetic assessment performed here using separately measured results considered radar systems with low transmit power, thus allowing for deep notches to be realized. In actuality, the hardware implementation may seriously limit the achievable notch depth. As experimentally determined in [9], notch depths of about 50 dB were obtained using a solid state amplifier operated in a linear mode, which degraded to 45 dB when the amplifier was operated in saturation. Given that one may expect even greater distortion for tube amplifiers that achieve even higher powers, it can be inferred that high power radar systems may not be able to produce notch depths that completely avoid interference at all distances from the transmitter. That said, efforts involving hardware-in-the-loop waveform optimization [16,17] and waveform/transmitter co-design [18,19] could eventually address this limitation.

7 Conclusions

Both simulated and experimentally measured PRO-FMCW waveforms having spectral notches were investigated as a means to emit radar waveforms in a spectrum containing narrowband interference. Relative to the radar center frequency, different interference spectral locations were considered at different relative power levels. It was found that the use of spectral notches introduces a trade-space with regard to extended range sidelobes versus the achievable sidelobe floor; with these effects being dependent on the relative power levels and how near the interference is to the center of the radar band. Simply put, all else being equal, interference is generally less detrimental and easier to suppress the further it is from the center of the band.

Acknowledgements

This work was supported in part by the US Army Research Office under Grant #W911NF-15-2-0063. The authors would

also like to thank Mr. Patrick McCormick of the University of Kansas for his significant help in capturing the experimental measurements.

References

- [1] Federal Communications Commission. "National broadband plan," Available: <http://www.broadband.gov>.
- [2] H. Griffiths, L. Cohen, S. Watts, E. Mokole, C. Baker, M. Wicks, S. Blunt. "Radar spectrum engineering and management: technical and regulatory issues," *Proc. IEEE*, vol. 103, no. 1, pp. 85-102, Jan. 2015.
- [3] A. Martone, K. Sherbondy, K. Ranney, T. Dogaru. "Passive sensing for adaptable radar bandwidth," *IEEE Intl. Radar Conf.*, May 2015.
- [4] A. Martone, K. Ranney, K. Sherbondy. "Genetic algorithm for adaptable radar bandwidth," *IEEE Radar Conf.*, May 2016.
- [5] J. Jakabosky, S.D. Blunt, B. Himed. "Waveform design and receive processing for nonrecurrent nonlinear FMCW radar," *IEEE Intl. Radar Conf.*, May 2015.
- [6] J. Jakabosky, S.D. Blunt, B. Himed. "Spectral-shape optimized FM noise radar for pulse agility," *IEEE Radar Conf.*, May 2016.
- [7] S.W. Frost, B. Rigling. "Sidelobe predictions for spectrally-disjoint radar waveforms," *IEEE Radar Conf.*, May 2012.
- [8] J. Jakabosky, S.D. Blunt, A. Martone. "Incorporating hopped spectral gaps into nonrecurrent nonlinear FMCW radar emission," *IEEE CAMSAP Workshop*, Dec. 2015.
- [9] J. Jakabosky, B. Ravenscroft, S.D. Blunt, A. Martone. "Gapped spectrum shaping for tandem-hopped radar/communications & cognitive sensing," *IEEE Radar Conf.*, May 2016.
- [10] B. Ravenscroft, P.M. McCormick, S.D. Blunt, J. Jakabosky, J.G. Metcalf, "Tandem-hopped OFDM communications in spectral gaps of FM noise radar," *IEEE Radar Conf.*, May 2017.
- [11] S.D. Blunt, M. Cook, J. Jakabosky, J. de Graaf, E. Perrins. "Polyphase-coded FM (PCFM) radar waveforms, part I: implementation," *IEEE Trans. AES*, vol. 50, no. 3, pp. 2218-2229, July 2014.
- [12] T. Higgins, T. Webster, A.K. Shackelford. "Mitigating interference via spatial and spectral nulling," *IET RSN*, vol.8, no.2, pp.84-93, Feb. 2014.
- [13] M. Bartz. "Large-scale dithering enhances ADC dynamic range," *Microwave RF*, vol. 32, pp. 192-198, May 1993.
- [14] B.C. Brock. "The role of noise in analog-to-digital converters," *Sandia Nat. Lab. Report*, SAND96-2697, Nov. 1996.
- [15] C.T. Allen, S.N. Mozaffar, T.L. Akins. "Suppressing coherent noise in radar applications with long dwell times," *IEEE GRS Letters*, vol. 2, no. 3, pp. 284-286, July 2005.
- [16] S.D. Blunt, J. Jakabosky, M. Cook, J. Stiles, S. Seguin, E.L. Mokole. "Polyphase-coded FM (PCFM) radar waveforms, part II: optimization," *IEEE Trans. AES*, vol. 50, no. 3, pp. 2230-2241, July 2014.
- [17] D. Eustice, C. Latham, C. Baylis, R.J. Marks, L. Cohen. "Amplifier-in-the-loop adaptive radar waveform synthesis," *IEEE Trans. AES*, vol. 53, no. 2, pp. 826-836, Apr. 2017.
- [18] C. Baylis, L. Wang, M. Moldovan, J. Martin, H. Miller, L. Cohen, J. De Graaf. "Designing transmitter for spectral conformity: power amplifier design issues and strategies," *IET RSN*, vol. 5, no. 6, pp. 681-685, July 2011.
- [19] H. Griffiths, S. Blunt, L. Cohen, L. Savy. "Challenge problems in spectrum engineering and waveform diversity," *IEEE Radar Conf.*, Apr./May 2013.